Engineering Fracture Mechanics Vol. 35, No. 1/2/3, pp. 39–46, 1990
Printed in Great Britain.

0013-7944/90 $3.00 + 0.00
Pergamon Press plc.

RELATION OF CONCRETE FRACTURE TOUGHNESS TO ITS INTERNAL STRUCTURE

VICTOR C. LI† and JOAN HUANG‡
Department of Civil Engineering, Massachusetts Institute of Technology, Cambridge, MA 02139, U.S.A.

Abstract—When subjected to tensile loads, concrete failure often initiates at the interfacial defects between the mortar and coarse aggregates. The branching of an interfacial crack into the mortar may form a dominant crack which leads to the eventual fracture plane. A simplified model, accounting approximately the physical events experienced by such a dominant crack, is developed to relate the internal structure and mechanisms of deformations to the post-peak behavior and fracture toughness of concrete.

1. INTRODUCTION

CONCRETE is a very brittle material with low tensile bearing capacity. Compared to structural steel, concrete has only 0.1 to 1% of its tensile strength, and only 0.2 to 4% of its fracture toughness. For this reason, while concrete structures are often reinforced and/or prestressed, tensile failure can often occur.

The internal structure of concrete on the 'meso' level is made up of cement paste, fine aggregate, large or coarse aggregates and air voids in the paste. Although cracking may start from voids in the paste, it is generally accepted that in normal concrete, the mortar/aggregate interface provides the weakest link which limits the strength of the material. This is because of the existence of bond cracks caused by bleeding, usually on the lower side of the aggregate in concrete placements[1]. In addition, Slate and Matheus[2] found that cement shrinkage during setting and hardening can induce bond cracks. In normal concrete, it has been found[3] that the bond strength is only 33 to 67% of the mortar tensile strength. These bond cracks provide natural flaw sites to initiate interfacial cracks which may subsequently branch into the cement matrix. Observations of interfacial cracks has been made by many researchers[1, 4]. Although bond cracks can limit the strength of the material, they can also provide mechanisms of crack deflection, arrest, blunting and branching when matrix cracks run near or into the interface between mortar and coarse aggregates[1]. This is reflected in the tortuosity of the fracture plane in concrete resulting in a toughness higher than that of mortar. These observations suggest that the coarse aggregate volume fractions and size, and the mortar/aggregate interfacial strength must contribute significantly to the material tensile properties.

This paper presents a model relating the internal structure and inelastic deformation mechanisms of concrete to its macroscopic post-peak tensile behavior analytically. A complete analysis of the tensile behavior, including the pre-peak nonlinear behavior of concrete, and the implications of the analysis to concrete materials engineering is reported elsewhere[5]. The most important concept employed here is that the tensile strength of concrete is limited by the branching of the largest interfacial crack into the mortar matrix, which forms a dominant crack. This dominant crack subsequently propagates into a 'homogeneous' material with an effective toughness which reflects the distribution of interfacial cracks at mortar/aggregate sites, and which reflects the possible deflection of the dominant crack when it intercepts the coarse aggregates. These concepts lead to the development of a post-peak tension-softening curve[6, 7] which accounts for the aggregate volume fraction and maximum aggregate size, and the mortar toughness. It has been shown [e.g. 6, 8] that the area under the tension–softening curve (the σ–δ curve) can be related to the fracture toughness of concrete. In the following, we present the essence of the analytic model (the details can be found in[5]), followed by a discussion of the model predictions with some experimental data of concrete post-peak behavior available in the literature. It is found that, with

†Associate professor of Civil Engineering; ‡Graduate student of Civil Engineering.

reasonable values for model parameters (not all of them are readily available), typical post-peak behavior of concrete can be predicted to be consistent with experimental observations.

2. THEORETICAL MODEL

2.1. *The post-peak tension–softening curve*

Consider the interfacial crack at a single mortar/aggregate interface, with the aggregate modelled as a circular disk, as in[9, 10, 11], shown as the inset in Fig. 1. Assuming that $K_{IC}^{if} < K_{IC}^{m} < K_{IC}^{agg}$ (K_{IC}^{if} = interfacial toughness; K_{IC}^{m} = mortar matrix toughness; K_{IC}^{agg} = coarse aggregate toughness), valid for normal concrete[12, 13], the relation between the ambient tensile stress and the dimension of the interfacial crack, measured in terms of θ, has been worked out by Cherepanov and reported by Zaitsev[11], and is illustrated in Fig. 1. This figure shows that as the ambient tensile load increases, small interfacial defects will propagate unstably to nucleate an interfacial crack, corresponding to the negatively sloped portion for small θ. The interfacial crack will subsequently propagate stably until the condition for branching into the mortar matrix is met, corresponding to the positively sloped portion of the curves and the intersection with a new curve (with horizontal axis labelled as L/R_{max} in Fig. 1). At any given load, e.g. σ^*, Fig. 1 indicates that interfacial cracks in aggregates with size range R_{crit} to R_{max} will propagate stably and contribute to the inelastic deformation in the prepeak nonlinearity of the stress–strain curve[5]. This figure also shows that the interfacial crack for the maximum-sized aggregate requires the minimum load to branch into the mortar, and forms the dominant or critical crack. Subsequently, this dominant crack will propagate unstably, leading to the formation and development of the eventual failure plane of the concrete. We shall model the post-peak behavior of concrete based on the analyses of the propagation of this dominant crack.

If the dominant crack is approximated as a 2D flat crack in an infinite medium, the reduced tensile load bearing capacity of this concrete will then be governed by

$$\sigma\sqrt{\pi a} = K_{IC}^{eff} \tag{1}$$

where a is the total crack length including the maximum aggregate dimension $2R_{max}$ and the branch crack, and K_{IC}^{eff} is an 'effective' fracture toughness experienced by the dominant crack. The tensile strength ($a = 2R_{max}$ when $\sigma = f_t$) of the concrete will then be given by

$$f_t\sqrt{\pi R_{max}} = K_{IC}^{eff}. \tag{2}$$

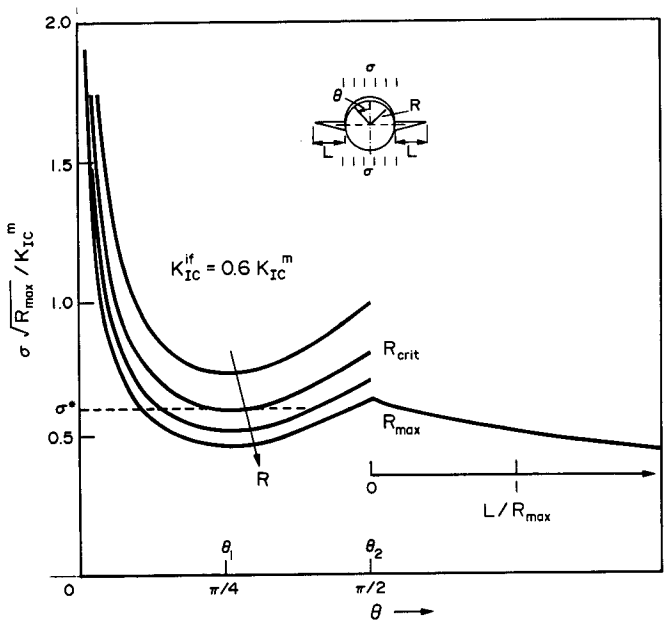

Fig. 1. Normalized ambient tensile stress vs interfacial crack angle θ based on[11].

In eqs (1) and (2) an effective toughness is used because the dominant crack is assumed to propagate into an effectively homogeneous material whereas the real concrete is highly inhomogeneous as seen by the dominant crack. The effective toughness of the material will be discussed in more detail below. For now, we recognize that as the dominant crack expands, the inelastic deformation in the concrete will be concentrated in this crack plane. Outside the plane of this dominant crack, the material will unload elastically.

The post-peak material separation δ at each load level σ may be estimated by smearing the crack opening area S over the total crack length. However, if we consider the physical process of the propagation of the dominant crack, it will be apparent that the total crack length for this calculation should be modified: the dominant crack will join with the interfacial crack each time it intercepts an aggregate. This leads to a jump of the dominant crack length by aggregate size $2R$, and should subsequently reduce the equilibrium load. However, the new crack tip resulting in the interfacial crack joining the dominant crack may be oriented in such a way that additional load will be required to reinitiate the dominant crack. For simplicity, we assume that these opposing effects cancel each other out approximately, so that the dominant crack jumps occur at essentially constant remote load.

To account for the dominant crack jump, an effective total crack length a_{eff} is introduced, which may be related to the averaged aggregate size and hence to the aggregate volume fraction[5]

$$a_{\text{eff}} = \frac{1}{1 - V_{\text{f}}} a. \tag{3}$$

The opening separation δ can now be related to the crack opening area S as:

$$\delta = \frac{S}{2a_{\text{eff}}} - \frac{S_0}{2a_{\text{eff}}} \tag{4}$$

where the second term is included to correct for the deformation already incurred at peak load, and where

$$S = \frac{2\pi\sigma}{E} (a_{\text{eff}})^2$$

$$S_0 = \frac{2\pi f_{\text{t}}}{E} \left(\frac{R_{\max}}{1 - V_{\text{f}}} \right)^2. \tag{5}$$

Thus combining eqs (1)–(5) we get an expression for the tension–softening curve:

$$\delta = \frac{(K_{\text{IC}}^{\text{eff}})^2}{E(1 - V_{\text{f}}) f_{\text{t}}} \frac{1}{\left(\frac{\sigma}{f_{\text{t}}} \right)} \left[1 - \left(\frac{\sigma}{f_{\text{t}}} \right)^3 \right]. \tag{6}$$

Apart from the $1/(1 - V_{\text{f}})$ term, the aggregate volume fraction also affects the tension–softening curve through f_{t} and $K_{\text{IC}}^{\text{eff}}$. The tensile strength f_{t} is in turn controlled by $K_{\text{IC}}^{\text{eff}}$ and by $R_{\max}$ through eq. (2). The critical energy release rate for the concrete may be obtained as the area under the tension-softening curve by integrating eq. (6). It should be noted that the σ–δ curve as expressed in eq. (6) has a long tail decaying indefinitely to $\sigma = 0$ as $\delta \to \infty$. What is likely to happen, in reality, is that the dominant crack representation of the deformation mode breaks down at large δ. Instead, a frictional pull-out mode takes over, and the analysis leading to eq. (6) becomes invalid. This frictional pull-out behavior is modelled in[5].

2.2. *Effective toughness for the dominant crack*

We now turn our attention to the calculation of the effective toughness $K_{\text{IC}}^{\text{eff}}$ experienced by the dominant crack. Conceptually when the dominant crack intercepts a coarse aggregate, it would most likely deflect around the aggregate because the mortar/aggregate interface is weak[14]. Deflection reduces the stress intensity factor at the new tip because the deflected crack

tip orientation is no longer perpendicular to the applied load. Thus the material is effectively toughened. In addition to crack deflection toughening, the presence of cracks at the mortar/aggregate interfaces reduces the elastic modulus of the material ahead of the dominant crack, leading to a shielding effect on the stress intensity factor felt by the dominant crack tip[15]. Again, the material is effectively toughened. The analyses of these toughening effects allow us to explicitly relate the aggregate volume fraction to the effective toughness K_{IC}^{eff} above that of the mortar toughness K_{IC}^{m}. It should be noted that other toughening and damaging mechanisms not accounted for in the present modelling effort may be operational simultaneously. These include, for example, crack blunting when it runs into an air void, or discontinuous crack planes which subsequently link together, and which increase the fracture surface area. Modelling of the crack deflection mechanism and reduced elastic moduli mechanism due to interfacial cracks do, however, account at least partially for the observation of weak interfaces and for the observation of fracture plane turtuosity in normal concrete under static loading.

To estimate the amount of toughening due to interfacial cracks, we consider that the material ahead of the dominant crack tip continues to deform elastically but with a tensile elastic modulus lower than the uncracked material. Using the path independence of the J-integral between contours in and outside of a zone of crack tip material with reduced moduli E and ν, Evans and Faber[16] show that the stress intensity factor felt by the crack tip is reduced leading to an effective toughening of the material:

$$K_{IC}^{dic}/K_{IC}^{m} = \sqrt{E_m(1-\nu)/E(1-\nu_m)} \tag{7}$$

where K_{IC}^{dic} is the effective toughness when distributed cracking is present, and E_m and ν_m are the moduli of the uncracked material. For our problem, we will need to estimate the ratio E/E_m based on the interfacial crack sizes and the volume fraction of coarse aggregates. This is carried out by means of a self-consistent technique first employed by Budiansky and O'Connell[17] in treating elastic bodies with a distribution of randomly oriented flat cracks. By adapting their analysis to our 2D problem and for cracks with similar orientation (normal to the ambient tensile load direction), and by assuming that the size, shape and orientations of the cracks are uncorrelated, Huang and Li[5] show that the reduced Young's modulus may be expressed in terms of the aggregate volume fraction as

$$\frac{E}{E_m} = 1 - \frac{\pi^2}{16}(1-\nu^2)V_f. \tag{8}$$

Equation (8) already used the approximation that each aggregate has one interfacial crack of length $(\pi/4)R$. This is based on the fact that for $K_{IC}^{if}/K_{IC}^{m} = 0.6$ typical of normal concrete, the trough of the load versus interfacial crack angle curve in Fig. 1 is reached at approximately $\theta_1 = (\pi/4)$, and the assumption that all the interfacial cracks ahead of the dominant crack are loaded to this stage. In reality the interfacial crack lengths probably span a spectrum of $0 < \theta < \theta_2$. Combining eqs (7) and (8) gives the effective toughness of the concrete accounting for the distribution of interfacial cracks:

$$K_{IC}^{dic}/K_{IC}^{m} = \sqrt{\frac{1}{1-\frac{\pi^2}{16}V_f(1-\nu^2)}} \tag{9}$$

where it has been assumed that $\nu = \nu_m$. For $\nu = 0.25$ and $V_f = 0.1, 0.3, 0.5, 0.7$, $K_{IC}^{dic}/K_{IC}^{m} = 1.03, 1.10, 1.18, 1.29$.

The present consideration of crack deflection toughening in concrete is based on an analysis by Faber *et al.*[18] who studied the amount of toughness improvement due to initial crack deflection induced by second phase spherical inclusions in ceramic systems. Their analysis takes into account that the inclusions may be intercepted by the dominant crack at various angles, resulting in a range of all possible deflecting angles. (The deflecting angle is defined by the angle between the dominant crack and the deflected branch at the crack tip.) Extension of the deflected crack in the coplanar direction was considered to be governed by the requirement that the local strain energy release rate G attains the critical value G_C, related to the matrix toughness K_{IC}^{m}. The strain energy release rate,

averaged over all possible deflecting angles, was calculated by using a probabilistic analysis. The result is:

$$K_{IC}^{def}/K_{IC}^{m} = \sqrt{1.0 + 0.87\,V_f} \tag{10}$$

where K_{IC}^{def} is the effective toughness due to crack deflection. The volume fraction of inclusions, V_f, comes into the equation through the consideration of the probability of crack–aggregate interceptions. For $V_f = 0.1, 0.3, 0.5, 0.7$, $K_{IC}^{def}/K_{IC}^{m} = 1.04, 1.12, 1.20, 1.27$. The possibility that the progagating crack does not intersect the center of the aggregate has also been considered in the derivation of eq. (10).

The effective toughness as experienced by the dominant crack may now be obtained by combining K_{IC}^{dic} and K_{IC}^{def} from eqs (9) and (10). Thus

$$K_{IC}^{eff}/K_{IC}^{m} = \sqrt{1.0 + 0.87\,V_f}\sqrt{\frac{1}{1 - \frac{\pi^2}{16}V_f(1-\nu^2)}}. \tag{11}$$

For $\nu = 0.25$, $V_f = 0.1, 0.3, 0.5, 0.7$, $K_{IC}^{eff}/K_{IC}^{m} = 1.07, 1.23, 1.41, 1.64$, respectively. This implies that the dominant crack propagates into a 'homogeneous' material whose toughness is effectively 64% higher than the mortar matrix toughness, for a concrete with $V_f = 0.7$. This effective toughness is used in eq. (6) for calculating the tension–softening curve.

3. MODEL PREDICTIONS AND EXPERIMENTAL OBSERVATIONS

The tensile strength decreases with the maximum aggregate size R_{max} as indicated by eq. (2). Figure 2 shows this decrease for a fix volume fraction $V_f = 0.7$ and for mortar matrix toughness $K_{IC}^{m} = 0.25$, 0.3 and 0.35 MPa $\sqrt{m}$. The typical range of tensile strength from 1.5 to 3.5 MPa for normal concrete (with R_{max} typically in the range 5 to 20 mm) is also indicated. This figure also indicates that higher strength in concrete may be obtained by reducing the size of aggregates, and this condition is often observed in the practical production of high strength concrete. Equations (2) and (11) also implies an increase of tensile strength with volume fraction of aggregate, other things being equal. This increase is not unequivocal, although there are limited experimental data to support this for V_f in the range of 0.2 to 0.8[19].

The complete tension–softening curve expressed by eq. (6) is used to compute the curves shown in Fig. 3, for three different mortar matrix toughness. Parametric values for f_t, E and V_f have been chosen to be equal to the concrete tested experimentally for their post-peak behavior in a stable

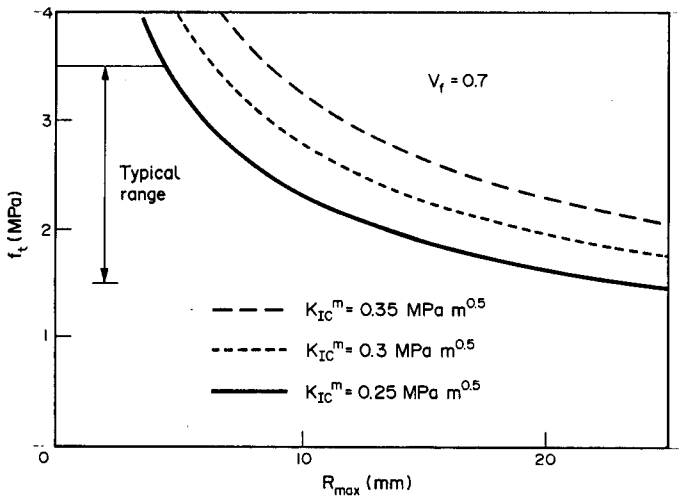

Fig. 2. Dependency of model predicted tensile strength on maximum aggregate size, and typical range of f_t for normal concrete. The higher values are usually obtained from split tension test, and lower values from direct tension test.

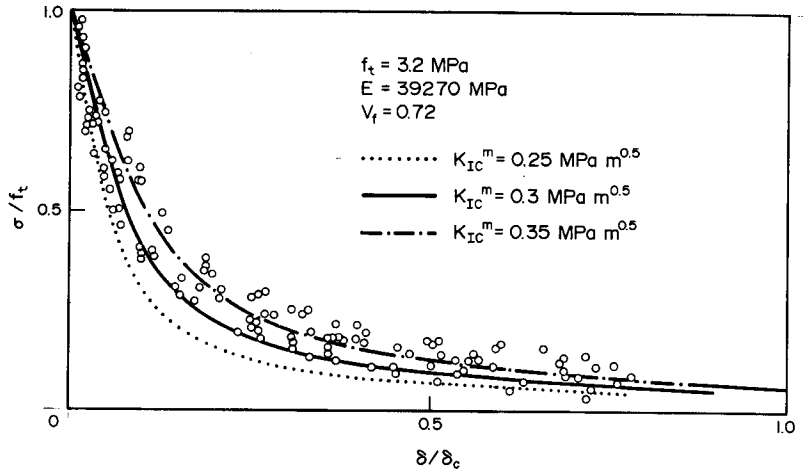

Fig. 3. Comparison of predicted and measured normalized tension-softening curve for a typical concrete. The experimental data is from[20].

direct tension test using a feed-back control loading frame[20]. The experimental data are also shown in Fig. 3. In spite of the many assumptions built into the theoretical model, the consistency between theoretical prediction (especially for the curves with larger values of K_{IC}^m) and experimental data is quite remarkable.

In real concrete mix design, the aggregate volume fraction and the maximum aggregate size are not independent variables. The amount of aggregates varies with the maximum aggregate size in order to maintain reasonable workability. Based on the mix design code given by[21], the predicted changes in tensile strength f_t and critical energy release rate G_c with maximum aggregate size D_{max} $(=2R_{max})$ is shown in Fig. 4(a) and (b). These figures suggest that while reducing the maximum aggregate size improves the tensile strength, there is also a simultaneous trade off in the fracture toughness of the material. While measurements of fracture toughness in high strength concrete are not available, there has been a number of reports on the brittle behavior of this material[22, 23].

Limited experimental data on the variation of critical energy release rate G_c of normal concrete for various maximum aggregate size has been reported in[24], using two concrete material with different water/cement ratios. The data, shown in Fig. 5, has a significant amount of scatter, even though the general trend (indicated by the solid linear regression line for all experimental data points) is consistent with the trends predicted by the present model. The model predicted trends in Fig. 5 are based on the same mix design code mentioned earlier, and for three different mortar matrix toughness. The experimental data was obtained from equal sized notched beams based on the RILEM recommended G_F fracture test.

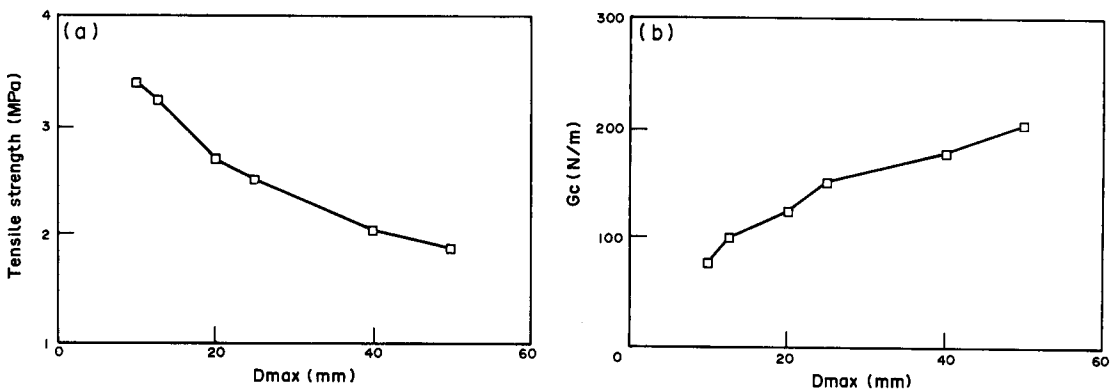

Fig. 4. (a) Model predicted tensile strength and (b) model predicted critical energy release rate, shown as a function of maximum aggregate size. The calculation is based on a concrete design mix code[21] which relates the volume fraction V_f to D_{max} for workability. Other parametric values used are: $\nu = 0.25$, $E = 24{,}000$ MPa, $K_{IC}^m = 0.3$ MPa $\sqrt{m}$ and a roughness parameter[5] $\eta = 10\,\mu m$.

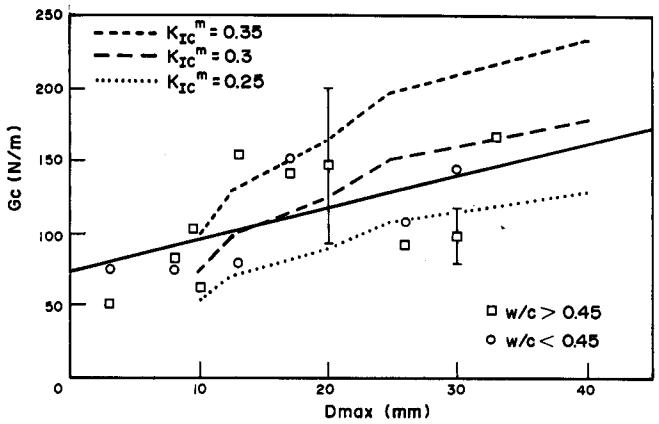

Fig. 5. Comparison of predicted and measured critical energy release rate as a function of maximum aggregate size. The experimental data is from[24]. See text for details.

4. CONCLUSIONS

The model presented is a much idealized picture of the complex processes of tensile failure in concrete. The simplified two dimentionality, the circular disk geometry of the coarse aggregates, the similar bond strength and nucleated interfacial crack angles at all mortar/aggregate interfaces, the simplified assumptions concerning the propagation of the dominant crack, amongst others, all contribute error to the analysis. In spite of these deficiencies, the model appears to predict essential features of tensile strength dependencies on R_{max} and V_f, and a post-peak tension–softening behavior and fracture toughness dependencies on R_{max} consistent with experimental results. Further, the model seems to provide some insight into the trade off between achieving high strength and fracture toughness, for conventional mix design. It should be noted, however, that the experimental data used in this paper do not serve to uniquely identify the physical mechanisms accounted for in the present model. Further work is required to eliminate or clarify the effects of some of the assumptions made in this simplified model. Extensions of this model to the nonlinear stage prior to peak load and comparisons with a wider range of experimental data will be reported in[5]. The main usefulness of the present work is to set the stage for a more refined study in relating the internal structure and deformation mechanisms to the composite properties. Current research in the effect of concrete additives such as microsilica or superplasticizers on the mortar/aggregate bond behavior and the mortar matrix toughness provides important tools in altering the properties of the internal structure of concrete. This combination of the availability of quantitative 'meso-mechanical' model and materials technology may be exploited for systematic and optimal materials engineering for high performance concrete.

Acknowledgements—The authors would like to thank A. Hillerborg and S. Mindness for many useful discussions. A grant from the National Science Foundation to MIT in support of this work is gratefully acknowledged.

REFERENCES

[1] F. O. Slate and K. O. Hover, Microcracking in concrete, in *Fracture Mechanics of Concrete* (Edited by A. Carpinteri and A. R. Ingraffea), pp. 137–159. Marhinus, Nijhoff, Dordrecht (1984).
[2] F. O. Slate and R. F. Matheus, Volume changes, on setting and curing of cement paste and concrete from zero to seven days. *J. Am. Concr. Inst. Proc.* **64,** 34–39 (1967).
[3] T. T. C. Hsu and F. O. Slate, Tensile bond between aggregate and cement paste or mortar. *J. Am. Concr. Inst. Proc.* **60,** 465–486 (1963).
[4] S. P. Shah and F. O. Slate, Internal microcracking, mortar–aggregate bond and the stress–strain curve of concrete, pp. 82–92. Cement and Concrete Association, London (1968).
[5] J. Huang and V. C. Li, A Meso-mechanical model of the tensile behavior of concrete. To be published in *Composites* (1989).
[6] A. Hillerborg, Analysis of one single crack, in *Fracture Mechanics of Concrete* (Edited by F. H. Wittmann), p. 223. Elsevier, Amsterdam (1983).
[7] V. C. Li and E. Liang, Fracture processes in concrete and fiber reinforced cementitious composites. *ASCE. J. Engng Mech.* **112,** 566–586 (1986).

[8] J. R. Rice, A path independent integral and the approximate analysis of strain concentrations by notches and cracks. *J. appl. Mech.*, 379–386 (1968).
[9] T. C. Y. Liu, A. H. Nilson and F. O. Slate, Stress–strain response and fracture of concrete in uniaxial and biaxial compression. *J. Am. Concr. Inst. Proc.* **69,** 291–295 (1972).
[10] A. K. Maji and S. P. Shah, A study of fracture process of concrete using acoustic emission, in *Proc. Soc. exp. Mech. Spring Conf.* Society for Experimental Mechanics (1986).
[11] Yu. V. Zaitsev, Inelastic properties of solids with random cracks, in *Mechanics of Geomaterials* (Edited by Z. Bazant), pp. 109–115. Wiley, New York (1985).
[12] B. Hillemeier and H. K. Hilsdorf, Fracture mechanics studies on concrete compounds. *Cement. Concr. Res.* **7,** 523–535 (1977).
[13] S. Ziegeldorf, Fracture mechanics parameters of hardened cement paste, aggregates and interfaces, in *Fracture Mechanics of Concrete* (Edited by F. H. Wittmann), pp. 371–409. Elsevier, Amsterdam (1983).
[14] S. P. Shah and F. J. McGarry, Griffith fracture criterion and concrete. *J. Engng Mech. Div. Proc. ASCE* **97,** 1663–1676 (1971).
[15] A. G. Evans and Y. Fu, Induced microcracking: effects of applied stress, in *Fracture in Ceramic Materials* (Edited by A. G. Evans), pp. 171–188. Noyes (1984).
[16] A. G. Evans and K. T. Faber, On the crack growth resistance of microcracking brittle materials, in *Fracture in Ceramic Materials* (Edited by A. G. Evans), pp. 109–136. Noyes (1984).
[17] B. Budiansky and R. J. O'Connell, Elastic moduli of a cracked solid. *Int. J. Solids Struct.* **12,** 81–97 (1976).
[18] K. T. Faber, A. G. Evans and M. D. Drory, A statistical analysis of crack deflection as a toughening mechanism in ceramic materials, in *Fracture Mechanics of Ceramics*, Vol. 6 (Edited by R. C. Bradt *et al.*), pp. 77–91. Plenum Press, New York (1983).
[19] A. F. Stock, D. J. Hannant and R. I. T. Williams, The effect of aggregate concentration upon the strength and modulus of elasticity of concrete. *Mag. Concr. Res.* **31,** 225–234 (1979).
[20] H. A. W. Cornelissen, D. A. Hordijk and H. W. Reinhardt, Experiments and theory for the application of fracture mechanics to normal and lightweight concrete, in *Fracture Toughness and Fracture Energy of Concrete* (Edited by F. H. Wittmann), pp. 565–575. Elsevier, Amsterdam (1986).
[21] A. M. Neville, *Properties of Concrete*, p. 700. Pitman (1981).
[22] S. Mindness, Relationships between strength and microstructure for cement-based materials: an overview, in *Very High Strength Cement-based Materials*, pp. 53–68. Material Science Research (1985).
[23] Y. S. Jeng and S. P. Shah, A measure for the fracture toughness of cement based materials, in *Very High Strength Cement-based Materials*, pp. 89–99. Material Science Research (1985).
[24] A. Hillerborg, Additional Concrete Fracture Energy Tests Performed By 6 Laboratories According to a Draft RILEM Recommendation. Report to RILEM, TC50-FMC, Lund, Sweden (1984).

(*Received for publication* 16 *November* 1988)